

Supporting Information

Achiral Substituents- and Stoichiometry-Controlled Inversion of Supramolecular Chirality and Circularly Polarized Luminescence in Ternary Co-Assemblies

Fang Wang*, Liyun Lai, Min Liu, Quan Zhou* and Shaoliang Lin*

School of Materials Science and Engineering, East China University of Science and Technology, Shanghai 200237, China.

E-mail: 1509wangfang@ecust.edu.cn (Fang Wang), qzhou@ecust.edu.cn (Quan Zhou), slin@ecust.edu.cn (Shaoliang Lin).

Experimental section

Materials

All reagents and solvents were used as received without further purification. Dimethyl sulfoxide (DMSO), Fmoc-*L*-phenylalanine (**L-Phe**), Fmoc-*D*-phenylalanine (**D-Phe**), Fmoc-*L*-leucine (**L-Leu**) and Fmoc-*D*-leucine (**D-Leu**) were purchased from Macklin. 3-(1-Naphthyl) acrylic acid (**NC1**), 3-(2-Naphthyl) acrylic acid (**NC2**), 4-(1-naphthylvinyl) pyridine (**NP**) and 1,2,4,5-tetracyanobenzene (**TCNB**) were purchased from Bore. All water used in this work was deionized water which obtained from Titan.

Preparation of assemblies

Self-assembly of different samples were triggered by a nanoprecipitation method. Taking the **L-Phe/NC1/TCNB** assemblies as an example, **L-Phe** (1.5 mg, 3.8 mmol), **NC1** (0.84 mg, 3.8 mmol) and **TCNB** (0.75 mg, 3.8 mmol) were dissolved in DMSO (50 μ L) by vigorous shaking in a septum-capped 5 mL glass vial. Then, by adding water (950 μ L) into the mixture, followed by aging at room temperature for at least 24 h, a yellow-color gel was eventually obtained, which was confirmed by the vial inversion test.

Characterization

UV-vis spectra were recorded on a Shimadzu UV-2600i spectrometer (Shimadzu, Japan) at room temperature in a 10 mm quartz cell. Fluorescence spectra were measured using a Perkin Elmer LS 55 spectrometer (Perkin Elmer, America). Circular dichroism (CD) and circularly polarized luminescence (CPL) spectra of the gel, suspension and solution samples were measured in quartz cuvettes (light path length 1 mm) on JASCO J-810 and JASCO CPL-300 spectrophotometers (JASCO, Japan), respectively. Scanning electron microscopy (SEM) was performed on a S-4800 microscope (Hitachi, Japan) with an accelerating voltage of 15 kV. One drop of the as-prepared gel or suspension samples was deposited on a polished silicon wafer, followed by drying and coating with a thin layer of Au to enhance the contrast. Fourier transform infrared (FTIR) spectra were measured on IRAffinity-1 Fourier infrared spectrometer (Shimadzu, Japan). Powder X-ray diffraction (XRD) data were measured on an Ultima IV X-ray diffractometer (Rigaku, Japan) operated in 2θ range from 3° to 30.0° at room temperature.

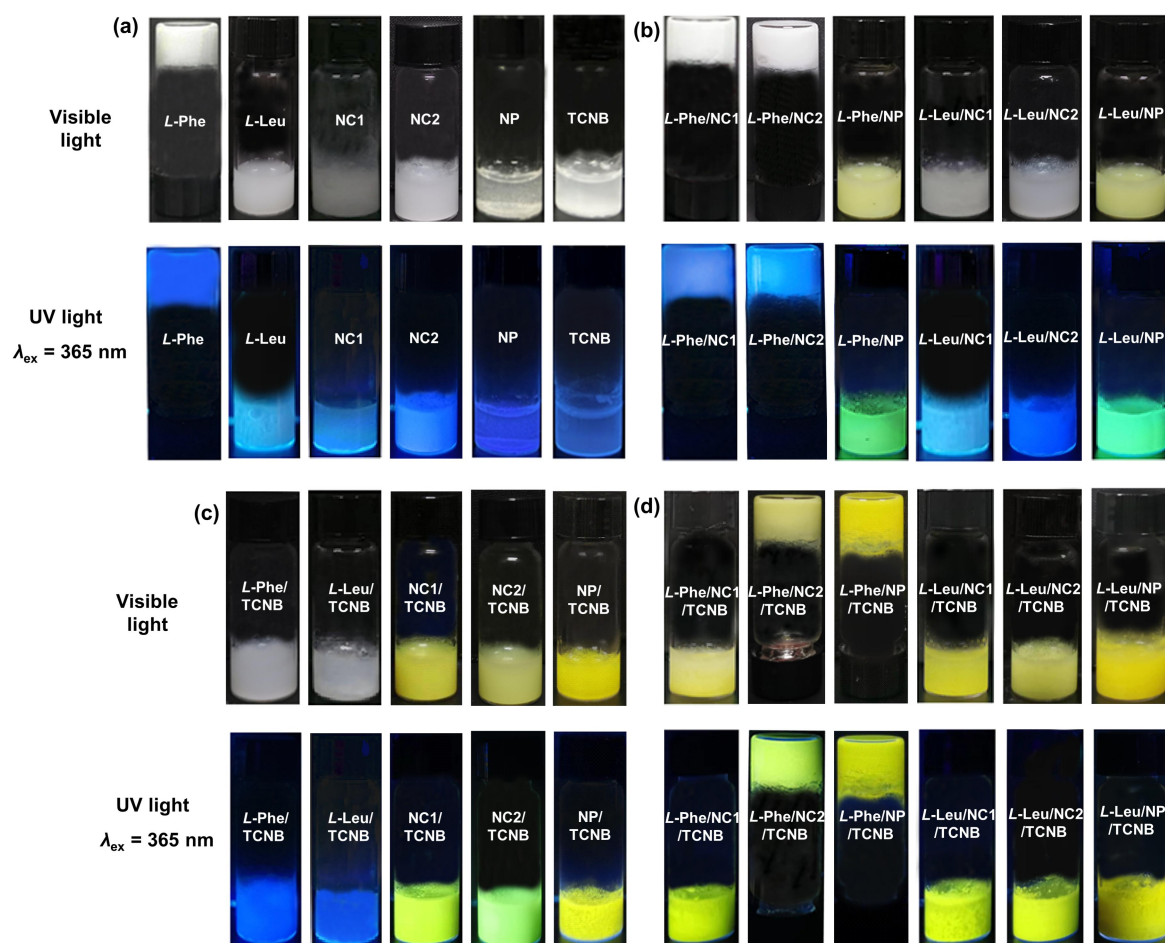


Fig. S1 Photographs of (a) individual *L*-Phe, *L*-Leu, NC1, NC2, NP and TCNB (3.8 mM) assemblies, binary assemblies of (b) *L*-Phe/NC1, *L*-Phe/NC2, *L*-Phe/NP, *L*-Leu/NC1, *L*-Leu/NC2 and *L*-Leu/NP (3.8 mM:3.8 mM), and (c) *L*-Phe/TCNB, *L*-Leu/TCNB, NC1/TCNB, NC2/TCNB and NP/TCNB (3.8 mM:3.8 mM), and (d) ternary assemblies of *L*-Phe/NC1/TCNB, *L*-Phe/NC2/TCNB, *L*-Phe/NP/TCNB, *L*-Leu/NC1/TCNB, *L*-Leu/NC2/TCNB and *L*-Leu/NP/TCNB (3.8 mM:3.8 mM:3.8 mM) formed in DMSO/H₂O (1/19, v/v) under visible light and UV light ($\lambda_{\text{ex}} = 365 \text{ nm}$).

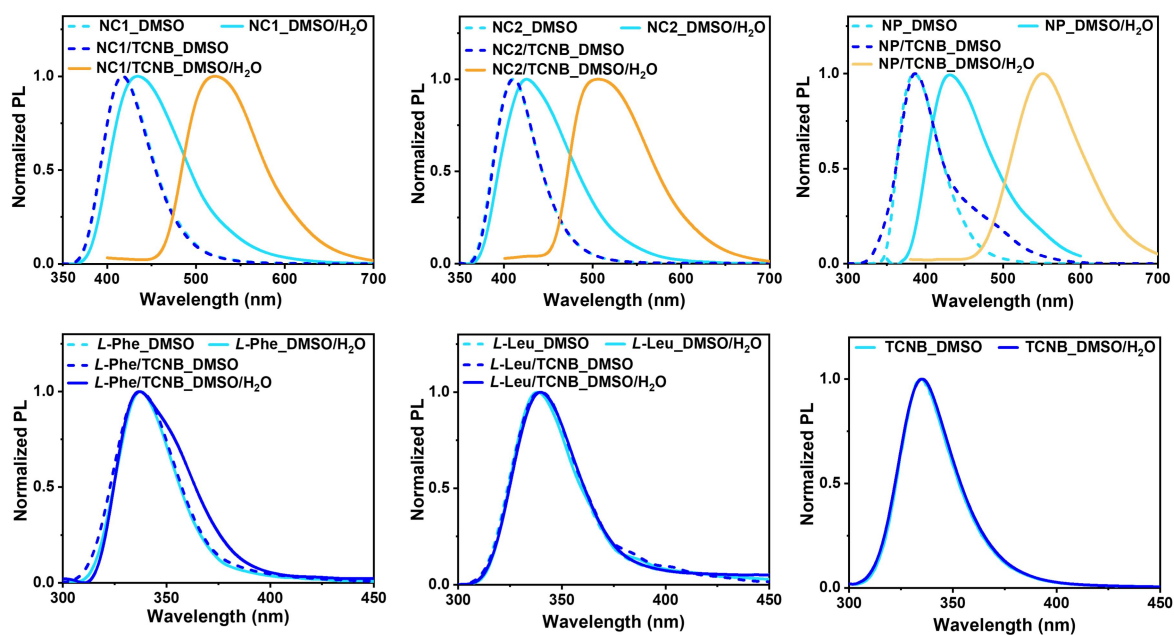


Fig. S2 Normalized PL spectra of individual *L-Phe*, *L-Leu*, **NC1**, **NC2**, **NP** and **TCNB** (3.8 mM) in DMSO ($\lambda_{\text{ex}} = 320$ nm for **NC1** and **NC2**, and $\lambda_{\text{ex}} = 280$ nm for **NP**, *L-Phe*, *L-Leu* and **TCNB**) and DMSO/H₂O ($\lambda_{\text{ex}} = 320$ nm for **NC1**, **NC2** and **NP**, and $\lambda_{\text{ex}} = 280$ nm for *L-Phe*, *L-Leu* and **TCNB**, 1/19, v/v), and **NC1/TCNB**, **NC2/TCNB**, **NP/TCNB**, *L-Phe/TCNB* and *L-Leu/TCNB* (3.8 mM:3.8 mM) in DMSO ($\lambda_{\text{ex}} = 320$ nm for **NC1/TCNB** and **NC2/TCNB**, and $\lambda_{\text{ex}} = 280$ nm for **NP/TCNB**, *L-Phe/TCNB* and *L-Leu/TCNB*) and DMSO/H₂O ($\lambda_{\text{ex}} = 360$ nm for **NC1/TCNB**, **NC2/TCNB** and **NP/TCNB**, and $\lambda_{\text{ex}} = 280$ nm for *L-Phe/TCNB* and *L-Leu/TCNB*, 1/19, v/v).

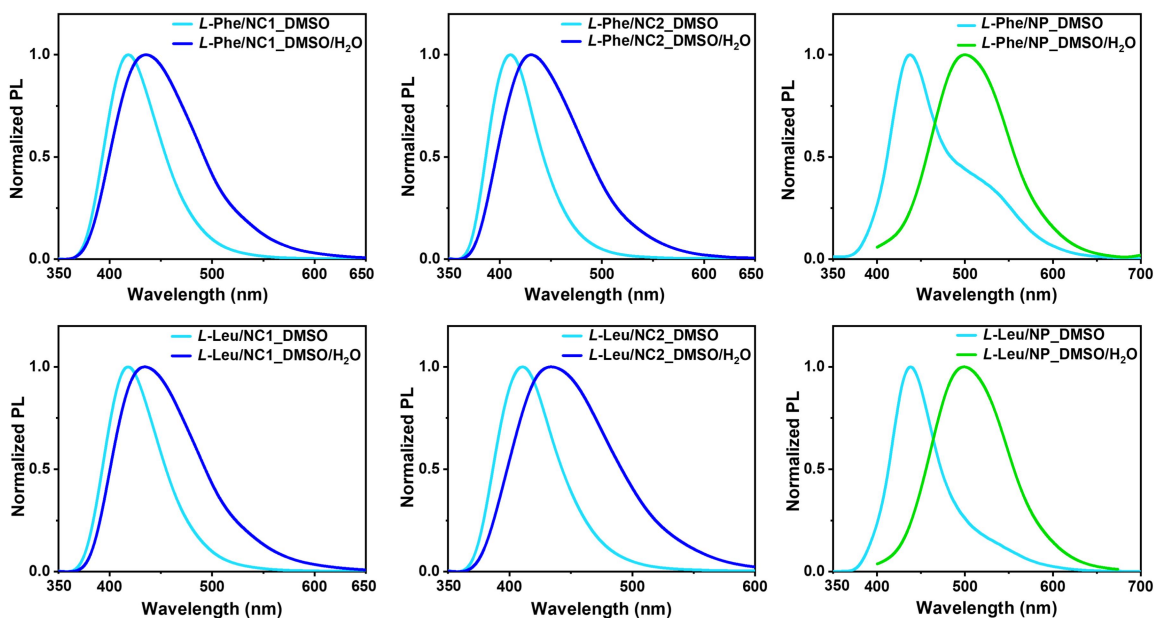


Fig. S3 Normalized PL spectra of *L-Phe/NC1*, *L-Phe/NC2*, *L-Phe/NP*, *L-Leu/NC1*, *L-Leu/NC2* and *L-Leu/NP* (3.8 mM:3.8 mM) in DMSO ($\lambda_{\text{ex}} = 320$ nm) and DMSO/H₂O ($\lambda_{\text{ex}} = 320$ nm for *L-Phe/NC1*, *L-Phe/NC2*, *L-Leu/NC1* and *L-Leu/NC2*, and $\lambda_{\text{ex}} = 360$ nm for *L-Phe/NP* and *L-Leu/NP*, 1/19, v/v).

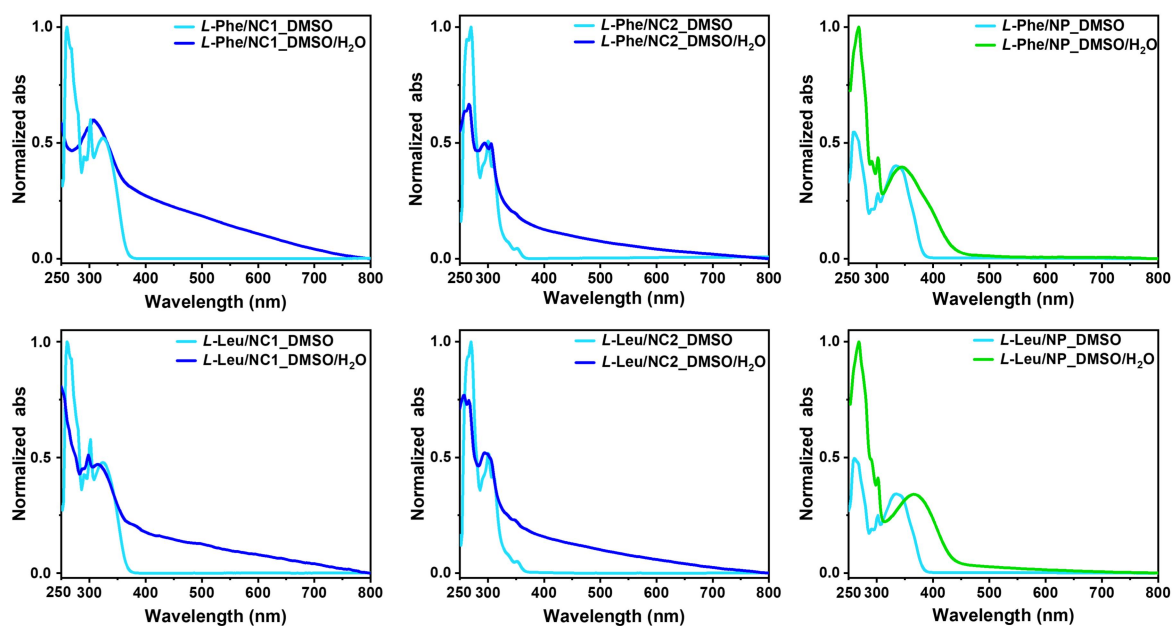


Fig. S4 Normalized UV-vis spectra of *L*-Phe/NC1, *L*-Phe/NC2, *L*-Phe/NP, *L*-Leu/NC1, *L*-Leu/NC2 and *L*-Leu/NP (3.8 mM:3.8 mM) in DMSO and DMSO/H₂O (1/19, v/v).

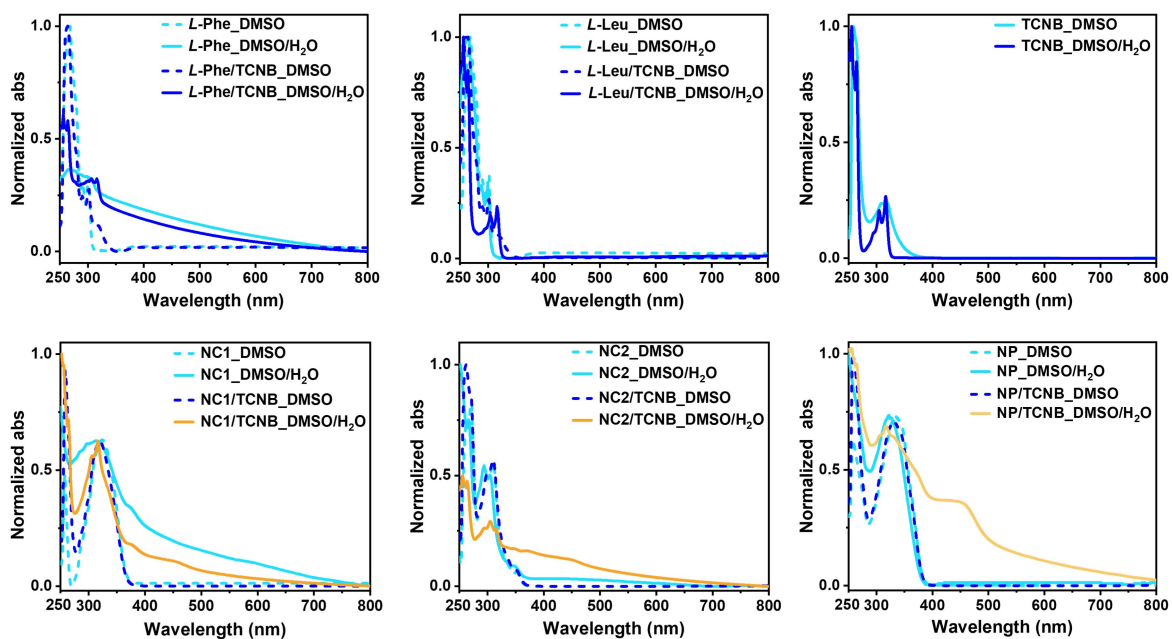


Fig. S5 Normalized UV-vis spectra of individual *L*-Phe, *L*-Leu, NC1, NC2, NP and TCNB (3.8 mM), and *L*-Phe/TCNB, *L*-Leu/TCNB, NC1/TCNB, NC2/TCNB and NP/TCNB (3.8 mM:3.8 mM) in DMSO and DMSO/H₂O (1/19, v/v).

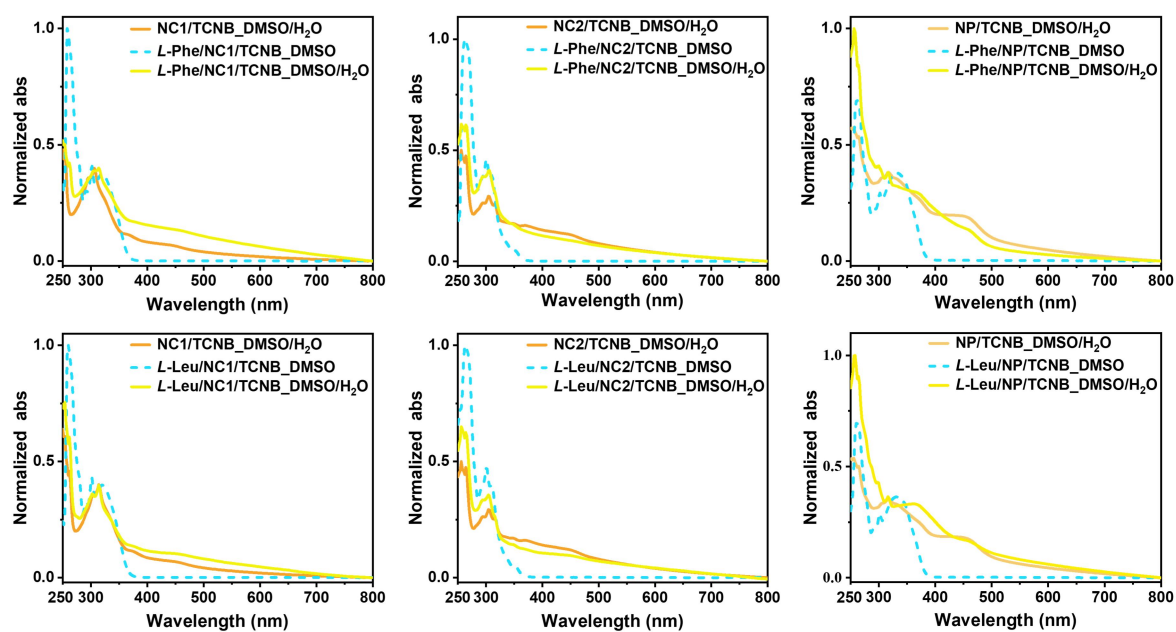


Fig. S6 Normalized UV-vis spectra of **NC1/TCNB**, **NC2/TCNB** and **NP/TCNB** (3.8 mM:3.8 mM) in DMSO/H₂O (1/19, v/v), and **L-Phe/NC1/TCNB**, **L-Phe/NC2/TCNB**, **L-Phe/NP/TCNB**, **L-Leu/NC1/TCNB**, **L-Leu/NC2/TCNB** and **L-Leu/NP/TCNB** (3.8 mM:3.8 mM:3.8 mM) in DMSO and DMSO/H₂O (1/19, v/v).

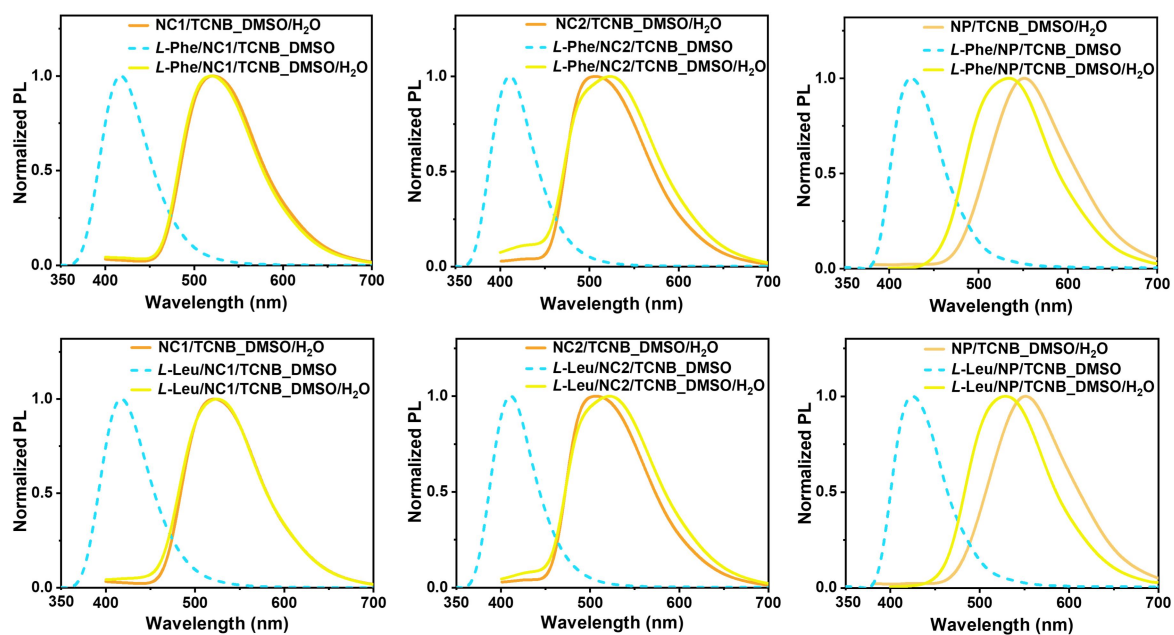


Fig. S7 Normalized PL spectra of **NC1/TCNB**, **NC2/TCNB** and **NP/TCNB** (3.8 mM:3.8 mM) in DMSO/H₂O ($\lambda_{\text{ex}} = 360$ nm, 1/19, v/v), and **L-Phe/NC1/TCNB**, **L-Phe/NC2/TCNB**, **L-Phe/NP/TCNB**, **L-Leu/NC1/TCNB**, **L-Leu/NC2/TCNB** and **L-Leu/NP/TCNB** (3.8 mM:3.8 mM:3.8 mM) in DMSO ($\lambda_{\text{ex}} = 320$ nm) and DMSO/H₂O ($\lambda_{\text{ex}} = 360$ nm, 1/19, v/v).

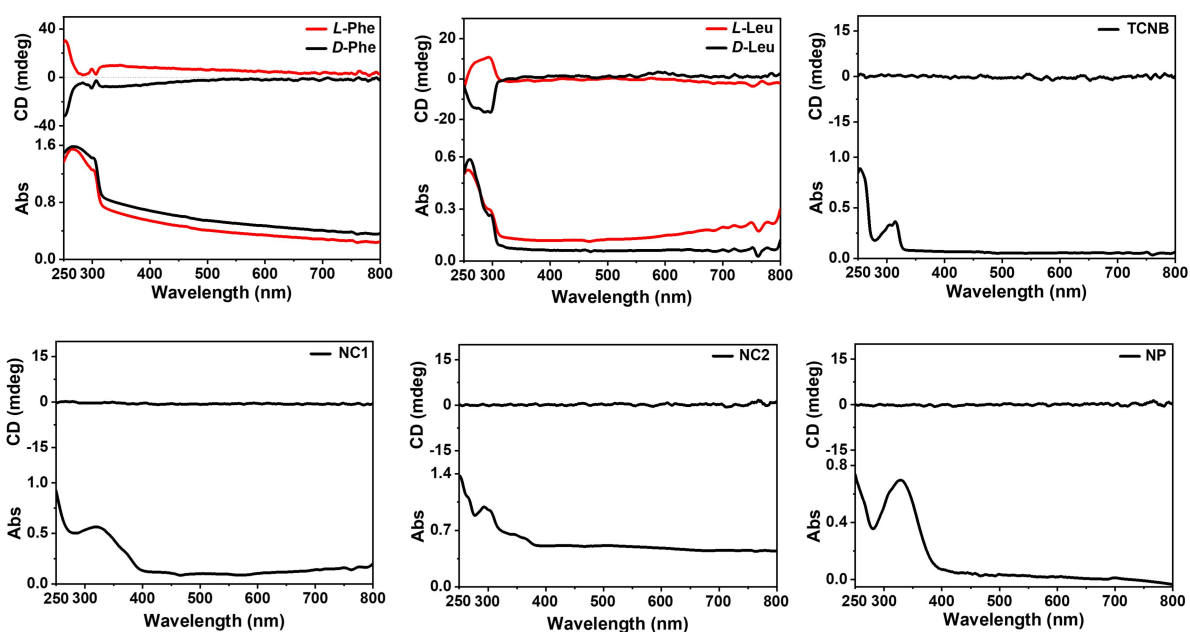


Fig. S8 CD and UV-vis spectra of individual *L*- or *D*-Phe, *L*- or *D*-Leu, NC1, NC2, NP and TCNB (3.8 mM) assemblies formed in DMSO/H₂O (1/19, v/v).

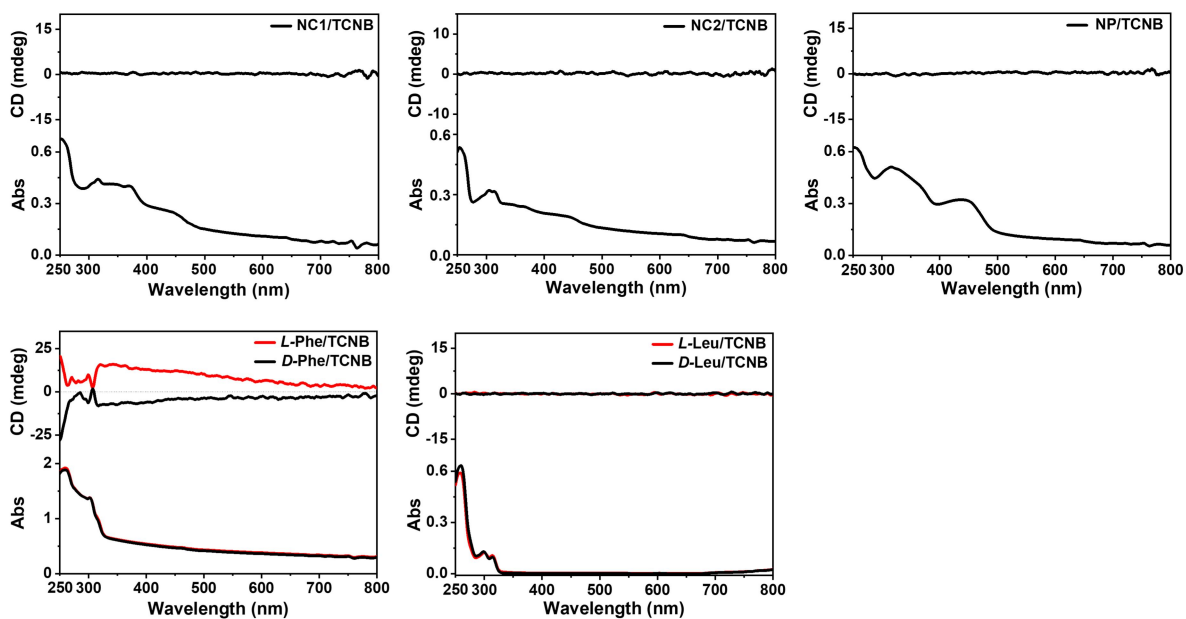


Fig. S9 CD and UV-vis spectra of NC1/TCNB, NC2/TCNB, NP/TCNB, *L*- or *D*-Phe/TCNB, and *L*- or *D*-Leu/TCNB (3.8 mM:3.8 mM) assemblies formed in DMSO/H₂O (1/19, v/v).

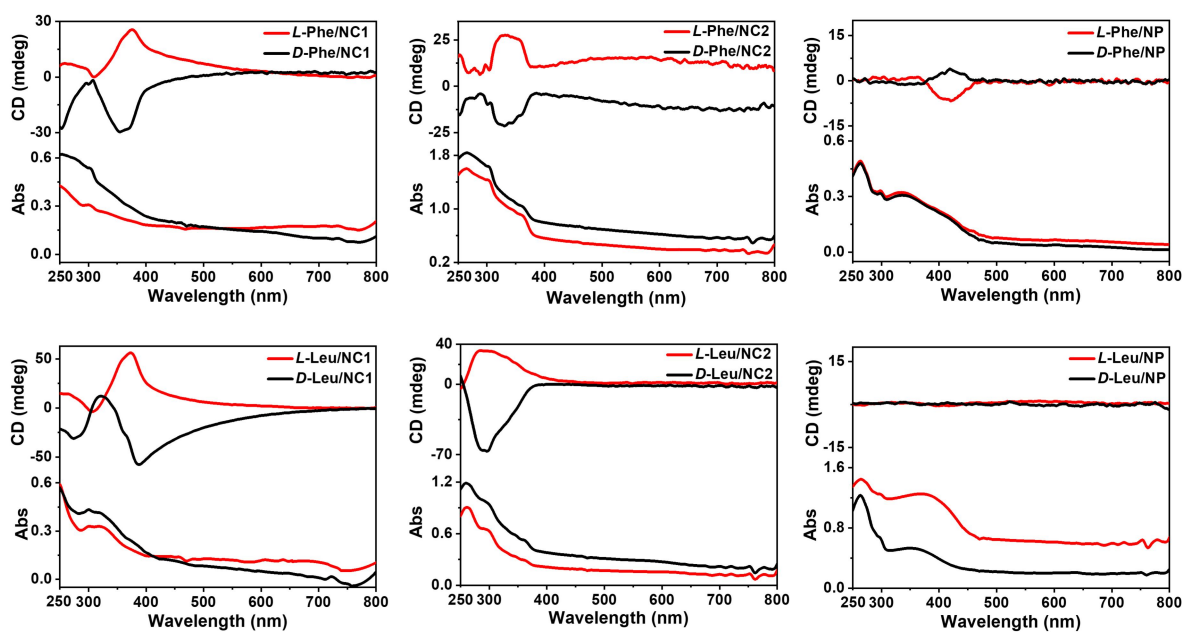


Fig. S10 CD and UV-vis spectra of *L*- or *D*-Phe/NC1, *L*- or *D*-Phe/NC2, *L*- or *D*-Phe/NP, *L*- or *D*-Leu/NC1, *L*- or *D*-Leu/NC2, and *L*- or *D*-Leu/NP (3.8 mM:3.8 mM) assemblies formed in DMSO/H₂O (1/19, v/v).

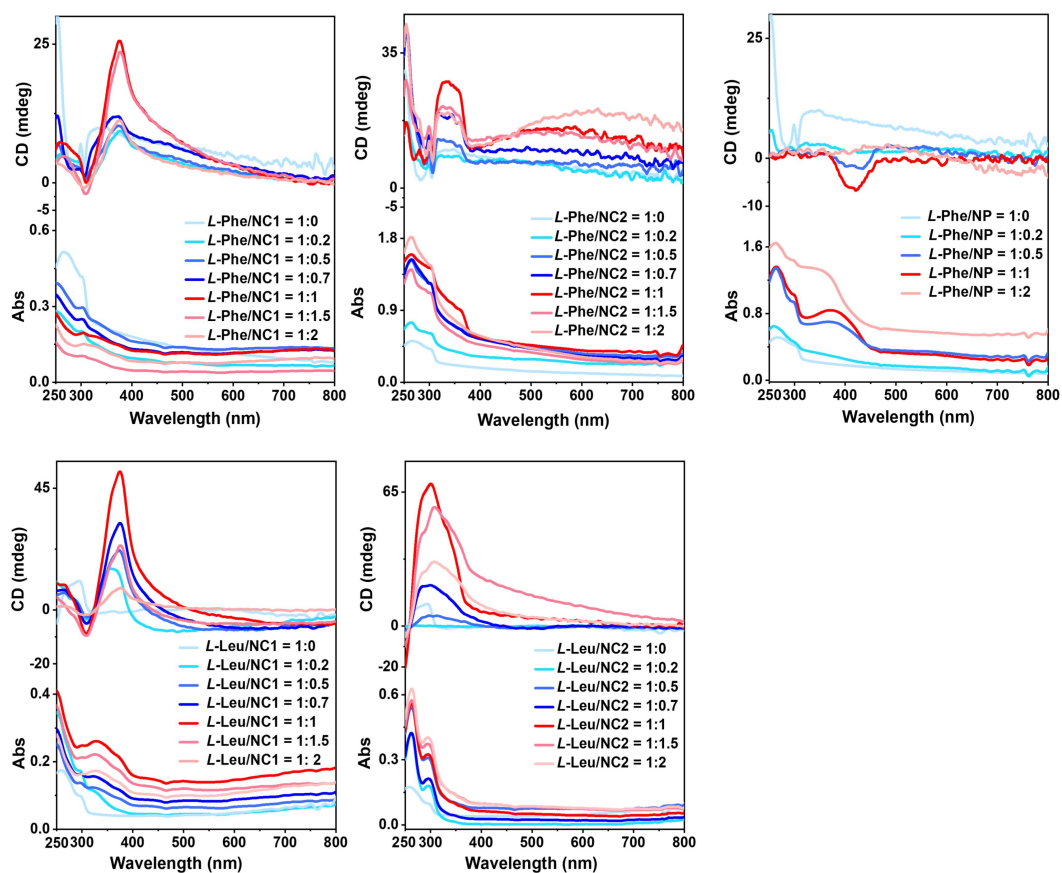


Fig. S11 Molar ratio-dependent CD and UV-vis spectra of *L*-Phe/NC1, *L*-Phe/NC2, *L*-Phe/NP, *L*-Leu/NC1 and *L*-Leu/NC2 in DMSO/H₂O (1/19, v/v).

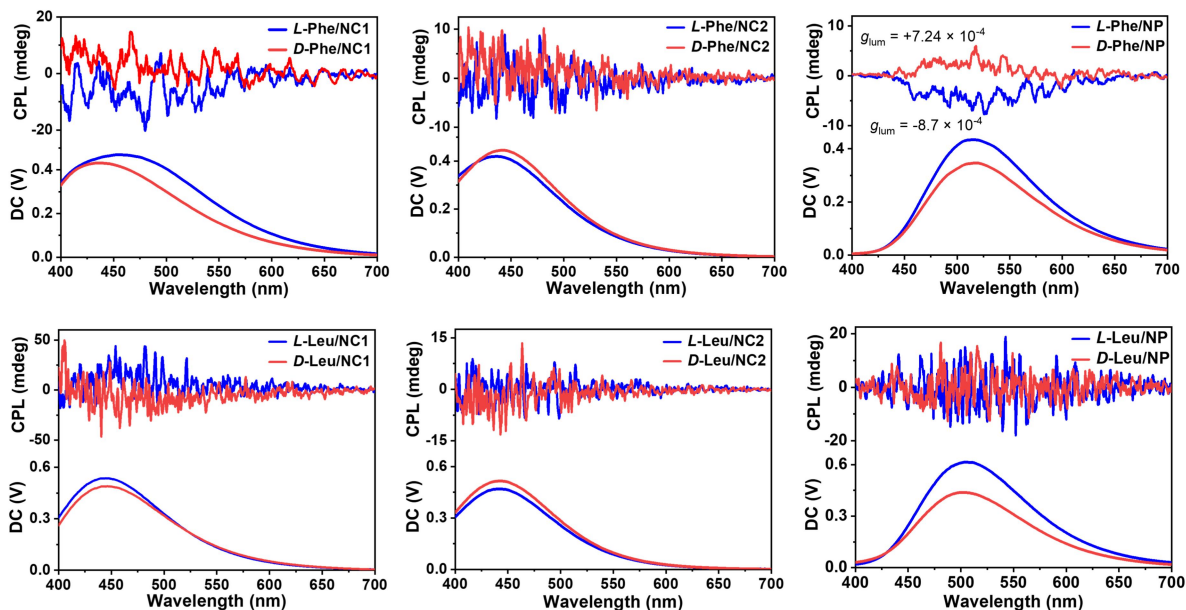


Fig. S12 CPL spectra of *L*- or *D*-Phe/NC1, *L*- or *D*-Phe/NC2, *L*- or *D*-Phe/NP, *L*- or *D*-Leu/NC1, *L*- or *D*-Leu/NC2, and *L*- or *D*-Leu/NP (3.8 mM:3.8 mM) in DMSO/H₂O (1/19, v/v) excited by 320 nm UV light.

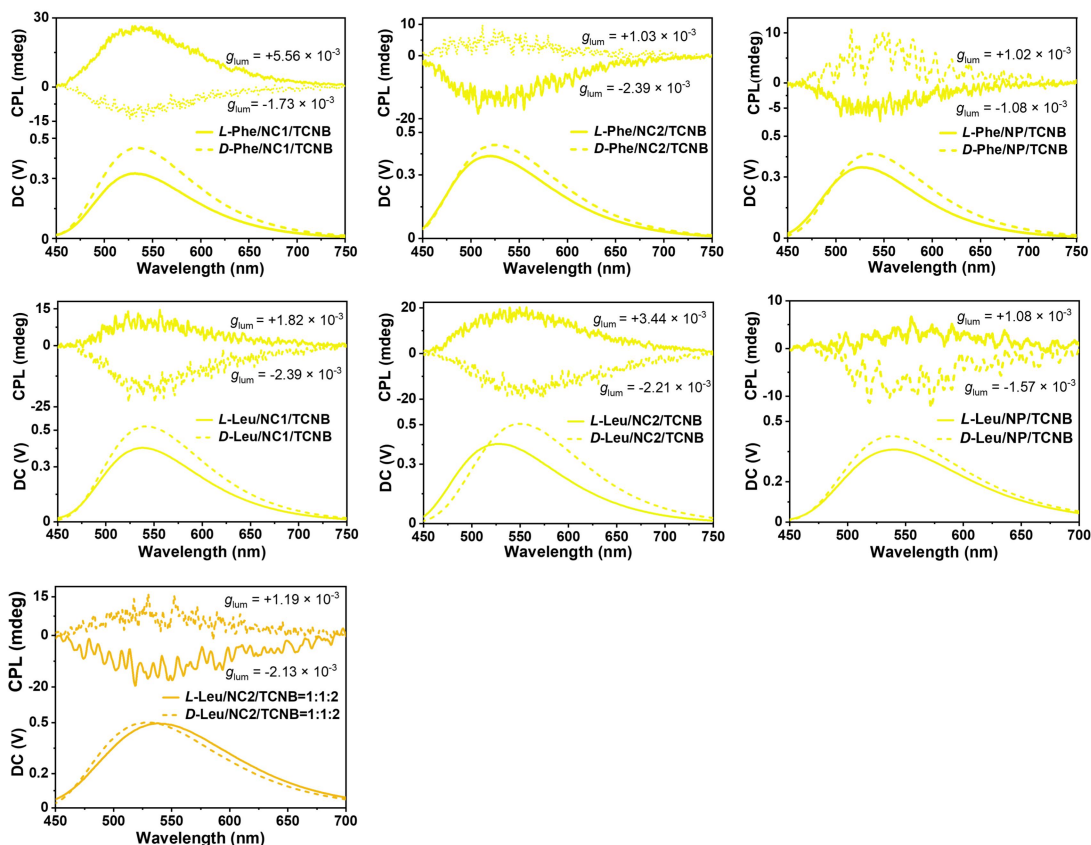


Fig. S13 CPL spectra of *L*- or *D*-Phe/NC1/TCNB, *L*- or *D*-Phe/NC2/TCNB, *L*- or *D*-Phe/NP/TCNB, *L*- or *D*-Leu/NC1/TCNB, *L*- or *D*-Leu/NC2/TCNB, *L*- or *D*-Leu/NP/TCNB (3.8 mM:3.8 mM:3.8 mM), and *L*- or *D*-Leu/NC2/TCNB = 1:1:2 (3.8 mM:3.8 mM:7.6 mM) in DMSO/H₂O (1/19, v/v) excited by 360 nm UV light.

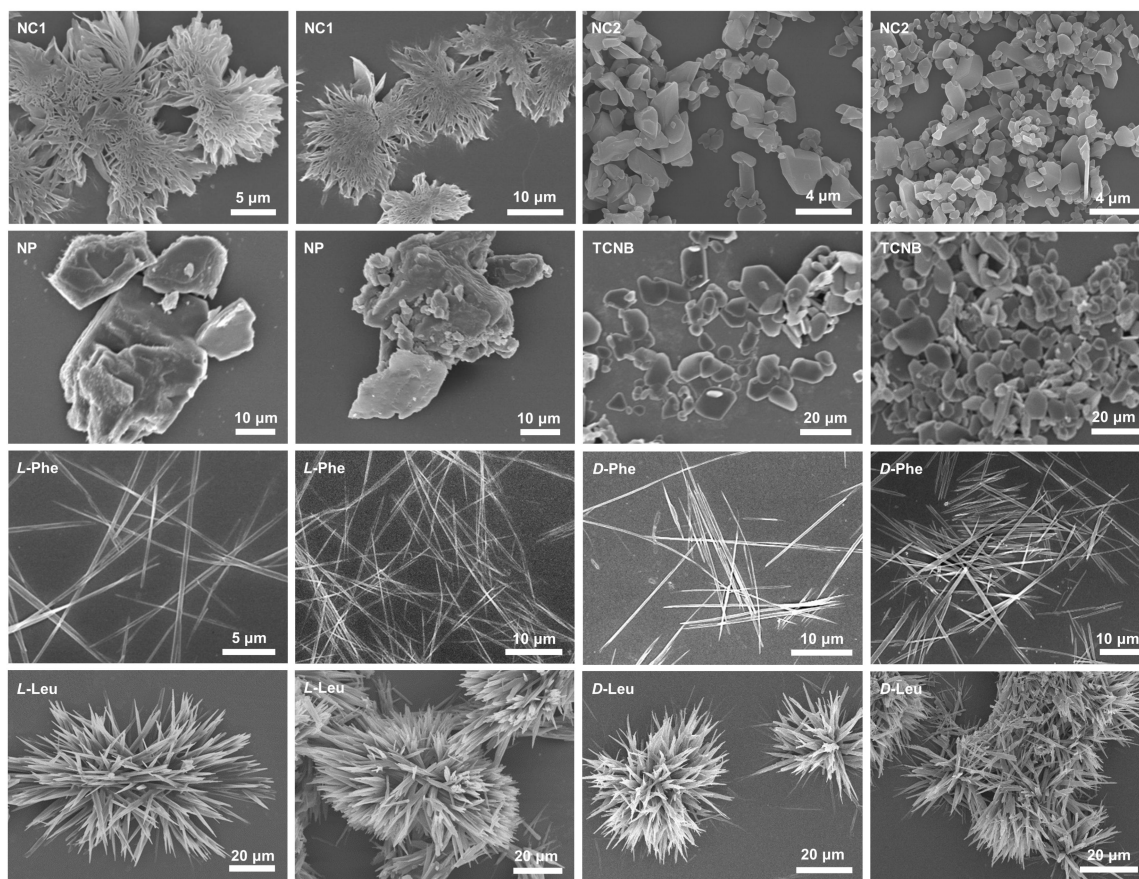


Fig. S14 SEM images of individual **NC1**, **NC2**, **NP**, **TCNB**, *L*- or *D*-**Phe**, and *L*- or *D*-**Leu** (3.8 mM) assemblies formed in DMSO/H₂O (1/19, v/v).

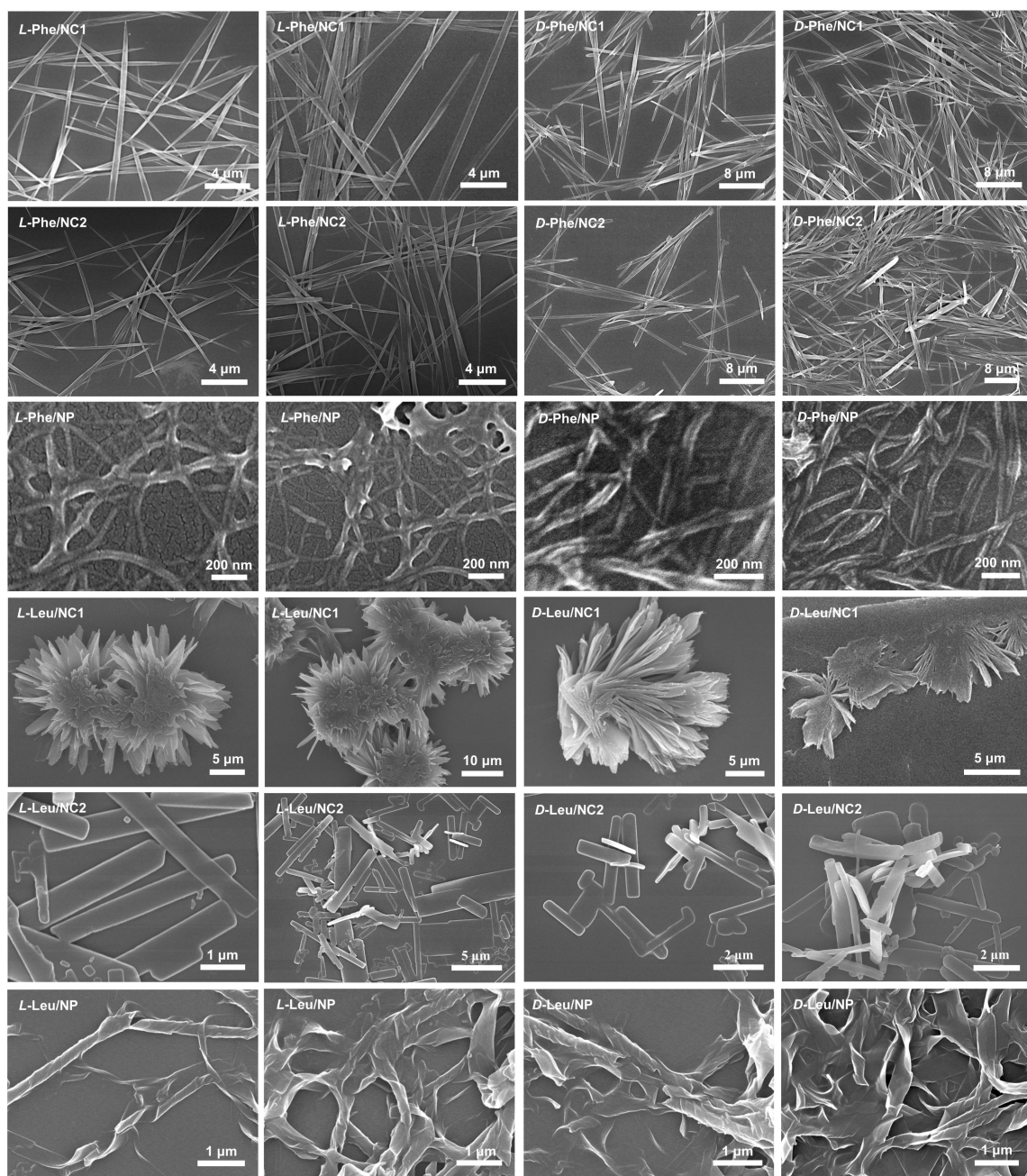


Fig. S15 SEM images of *L*- or *D*-Phe/NC1, *L*- or *D*-Phe/NC2, *L*- or *D*-Phe/NP, *L*- or *D*-Leu/NC1, *L*- or *D*-Leu/NC2, and *L*- or *D*-Leu/NP (3.8 mM:3.8 mM) assemblies formed in DMSO/H₂O (1/19, v/v).

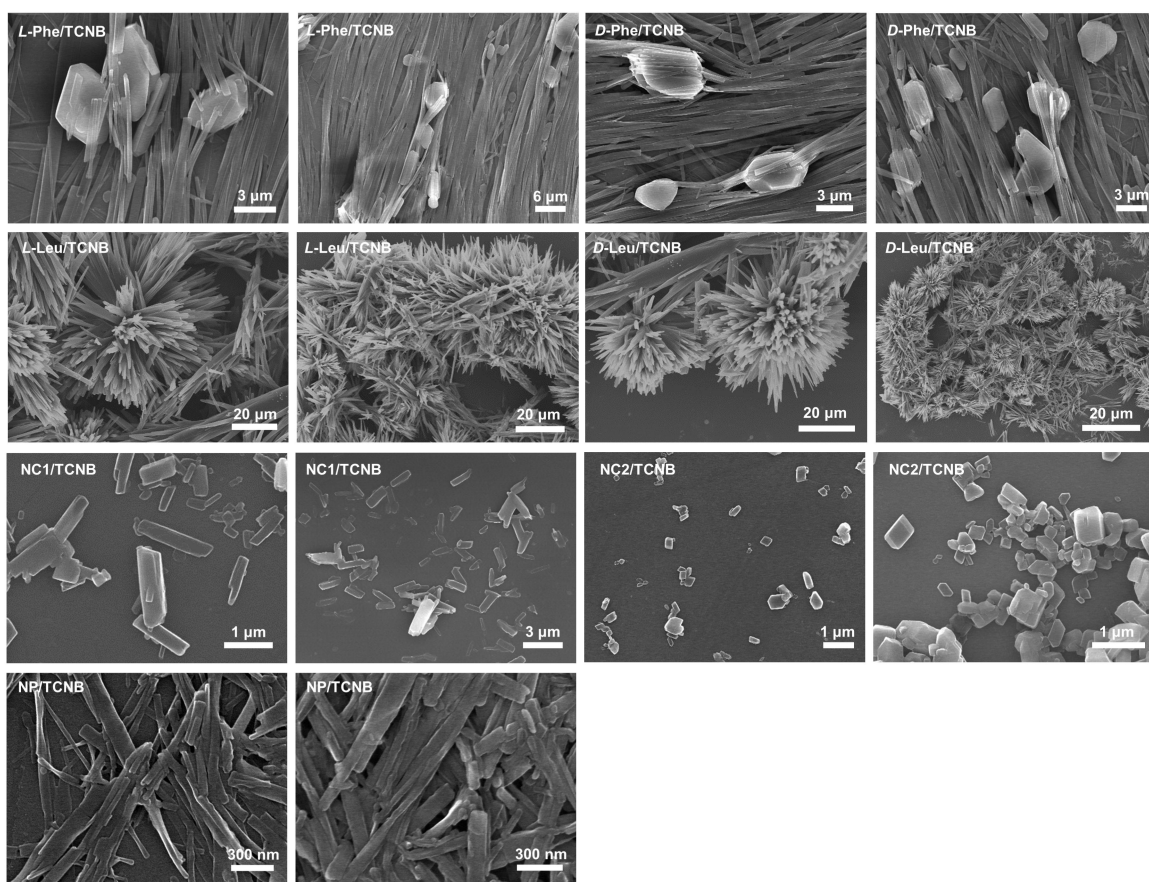


Fig. S16 SEM images of assemblies of *L*- or *D*-Phe/TCNB, *L*- or *D*-Leu/TCNB, NC1/TCNB, NC2/TCNB and NP/TCNB (3.8 mM:3.8 mM) formed in DMSO/H₂O (1/19, v/v).

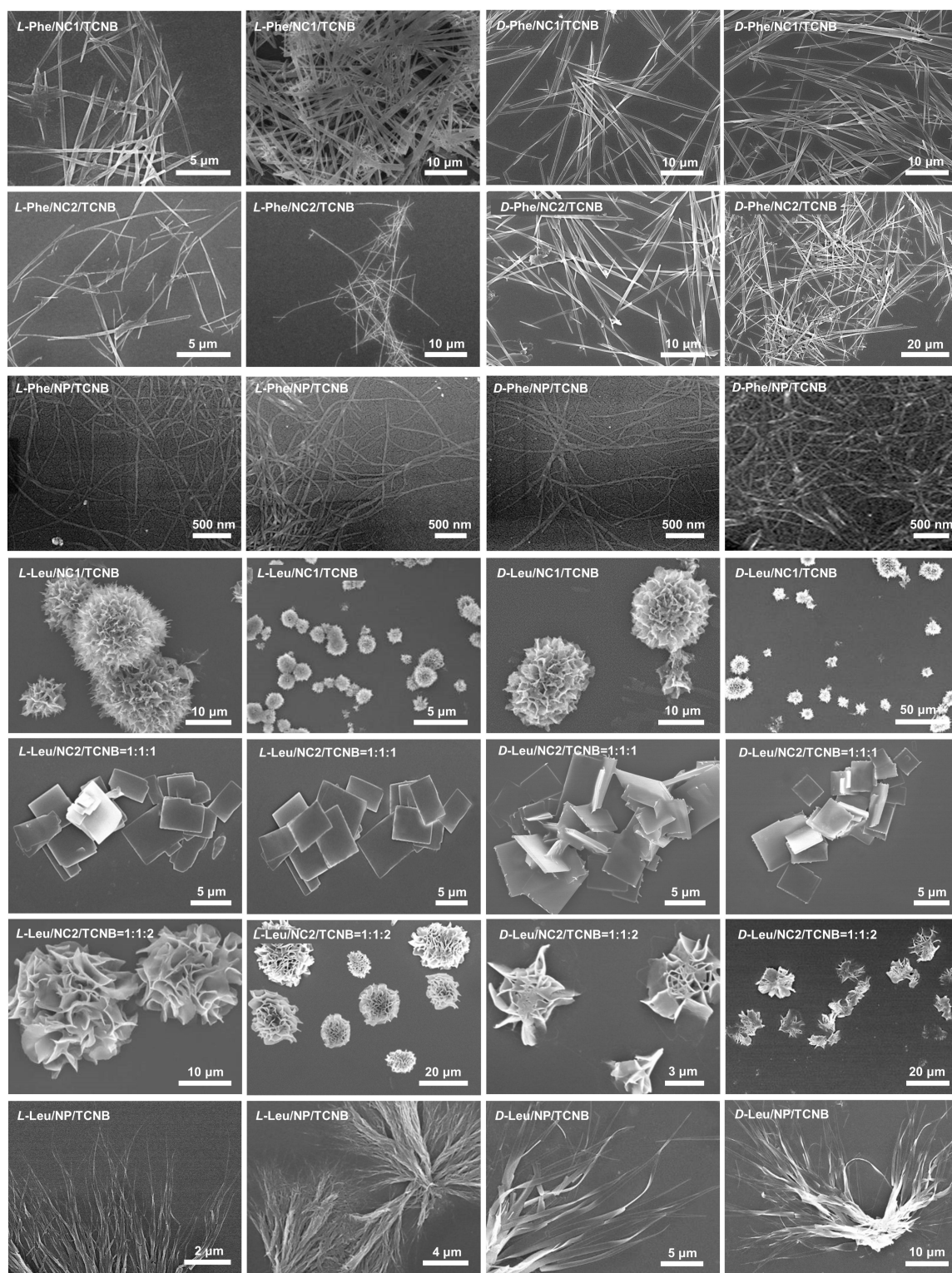


Fig. S17 SEM images of ternary assemblies of *L*- or *D*-Phe/NC1/TCNB, *L*- or *D*-Phe/NC2/TCNB, *L*- or *D*-Phe/NP/TCNB, *L*- or *D*-Leu/NC1/TCNB, *L*- or *D*-Leu/NC2/TCNB and *L*- or *D*-Leu/NP/TCNB (3.8 mM:3.8 mM:3.8 mM), and *L*- or *D*-Leu/NC2/TCNB = 1:1:2 (3.8 mM:3.8 mM:7.6 mM) formed in DMSO/H₂O (1/19, v/v).

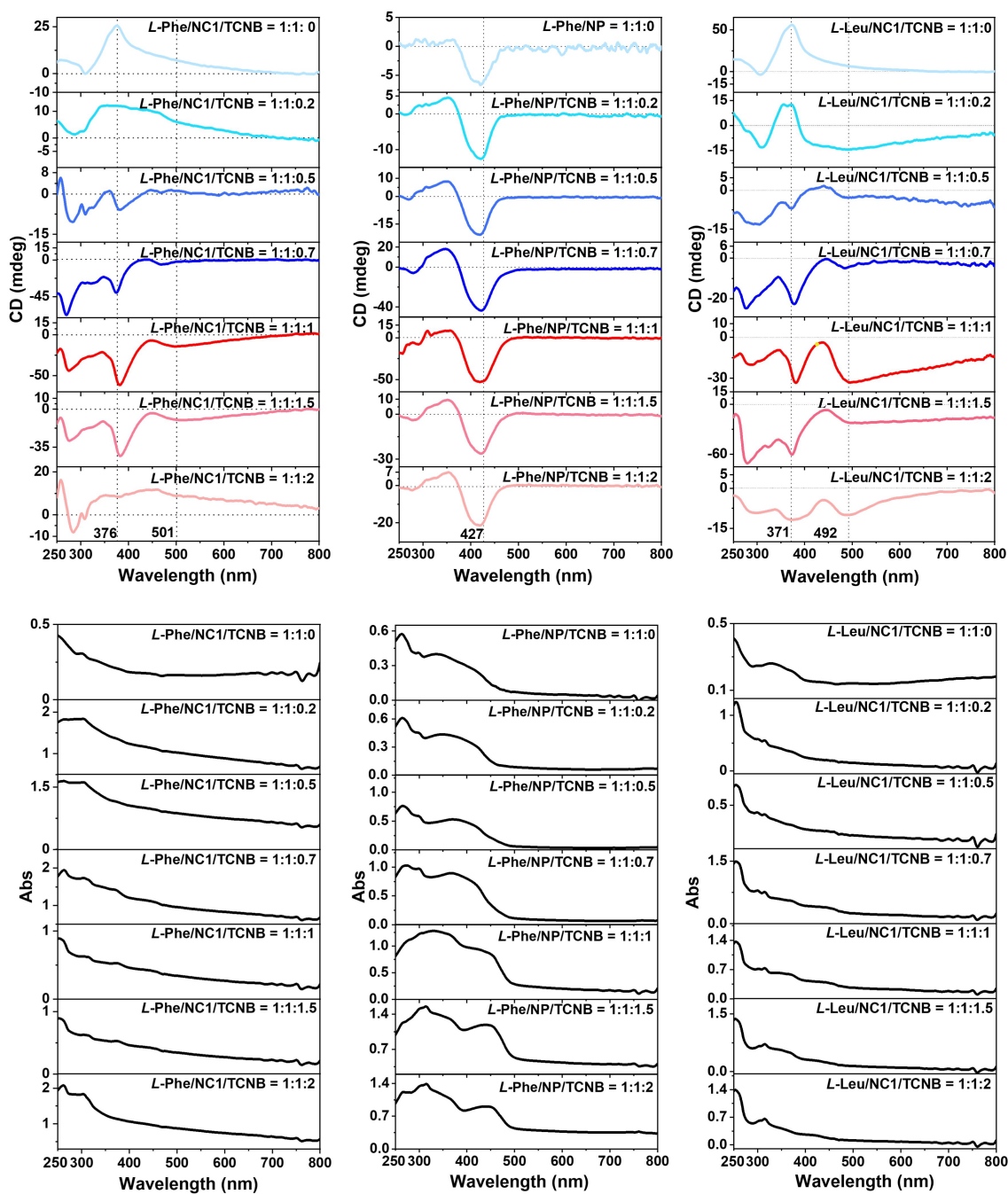


Fig. S18 Molar ratio-dependent CD and UV-vis spectra of *L*-Phe/NC1/TCNB, *L*-Phe/NP/TCNB and *L*-Leu/NC1/TCNB in DMSO/H₂O (1/19, v/v).

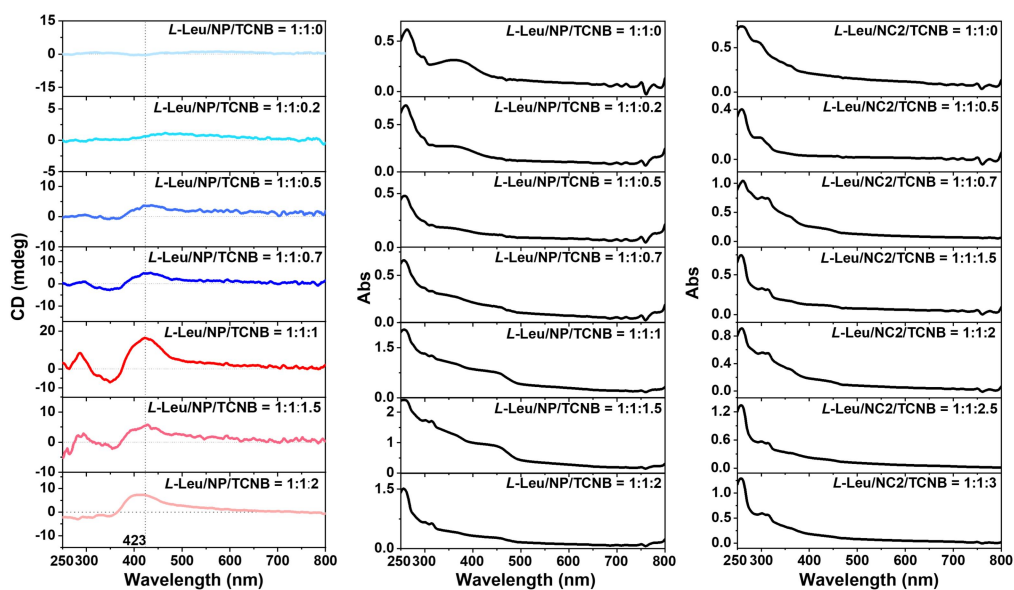


Fig. S19 Molar ratio-dependent CD and UV-vis spectra of *L*-Leu/NP/TCNB and molar ratio-dependent UV-vis spectra of *L*-Leu/NC2/TCNB in DMSO/H₂O (1/19, v/v).

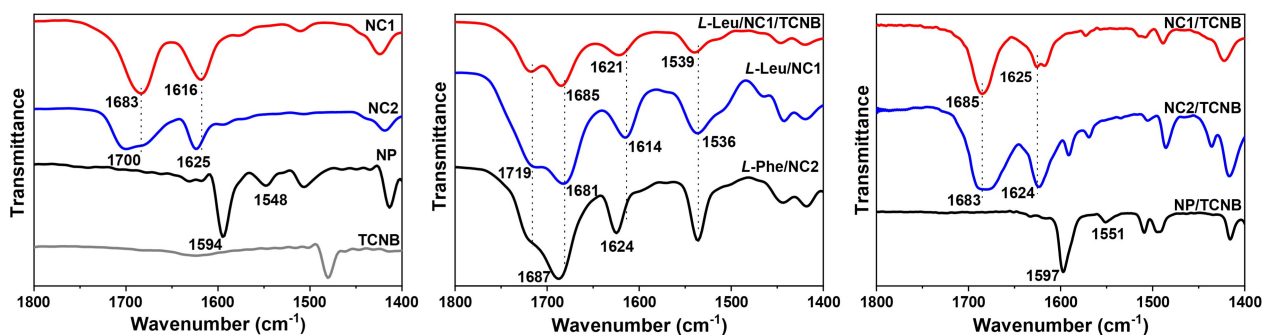


Fig. S20 FTIR spectra of individual NC1, NC2, NP and TCNB assemblies (3.8 mM), and assemblies of *L*-Phe/NC2, *L*-Leu/NC1, NC1/TCNB, NC2/TCNB and NP/TCNB (3.8 mM:3.8 mM), and *L*-Leu/NC1/TCNB (3.8 mM:3.8 mM:3.8 mM) formed in DMSO/H₂O (1/19, v/v).

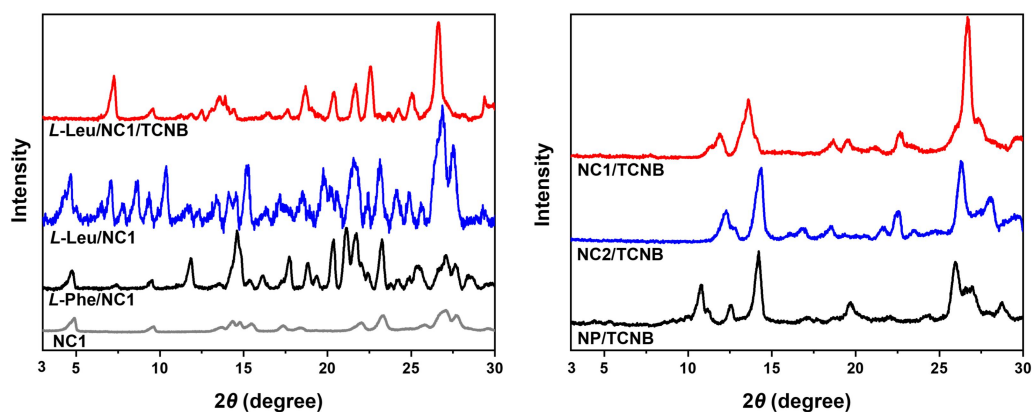


Fig. S21 Powder XRD patterns of assemblies of NC1 (3.8 mM), *L*-Phe/NC1, *L*-Leu/NC1, NC1/TCNB, NC2/TCNB and NP/TCNB (3.8 mM:3.8 mM), and *L*-Leu/NC1/TCNB (3.8 mM:3.8 mM:3.8 mM) formed in DMSO/H₂O (1/19, v/v).